Electronic Supplementary Material (ESI) for Green Chemistry.

Supporting information

A direct pathway for the coupling of arenes and alkylamines via a heterogeneous zeolite-based photocatalyst

Vincent Lemmens, Kwinten Janssens, Jorge Gascon and Dirk E. De Vos*

*Centre for Membrane Separations, Adsorption, Catalysis and Spectroscopy for Sustainable Solutions (cMACS), KU Leuven, Celestijnenlaan 200F p.o. box 2454, 3001 Leuven, Belgium.

E-mail: dirk.devos@kuleuven.be

Table of Contents

1. Materials and methods

General information

All commercially available compounds were used as received. Product quantification was performed on a Shimadzu CP-Sil 8 CB column together with a flame ionization detector. An Agilent 6890 gas chromatograph with a HP-1 MS colomn and a 6973 MSD mass spectrometer was used for the identification of the different products. Furthermore, ^{1}H-NMR spectra were collected for reaction/catalyst characterization with a Bruker AMX-300 spectrometer at 400 MHz (16 scans (^{1}H-NMR)) and data were analyzed using MestReNova 12.0.2 software package. Powder X-ray diffraction (PXRD) were recorded on a Malvern PANalytical Empyrean diffractometer equipped with a PIXcel 3D 1x1 detector. The powder samples were put onto a 96-well plate and patterns were recorded at room temperature in transmission geometry within a 1.3 °- 50 ° 2θ-range with a step size of 0.013° and analyzed via PANalytical Data Viewer software. The simulated patterns were simulated by Mercury 3.10 based on the corresponding CIF-files. The leached ruthenium content in solution and the ruthenium content in the zeolite after breakdown in aqua regia/HF were determined by inductively coupled plasma atomic emission spectroscopy (ICP-OES) using a Varian 720-ES. Fourier transform infrared spectroscopy (FTIR) was performed on a potassium bromide (FTIR grade, Sigma-Aldrich) pellet using a Nicolet 6700 spectrometer. UV-Vis data were collected for the homogeneous complex in an acetonitrile solution with a Thermoscientific Genesys 150 UV-Vis spectrometer. The UV-Vis spectrum for the complex encapsulated in the zeolite was collected with a CARY 5000 UV-Vis-NIR between 4000-50000 cm^{-1}. Nitrogen physisorption was performed on a Micrometrics 3Flex surface analyzer. Before measurement, the samples were activated at 200 °C for 16 h and surface areas were calculated by the multipoint Brunauer-Emmett-Teller (BET) method. Ru K-edge X-ray absorption spectroscopy (XAS) spectra were collected at the SUPERXAS beamline at Swiss light source (SLS) and analyzed with the Athena and Artemis software packages. Normalization of the data and background removal were performed in Athena; the X-ray absorption edge energy was calibrated using the spectrum of Ru^{0} foil and its integrated FEFF6 software was used for the extended X-ray absorption near edge surface (XANES) and X-ray absorption fine structure (EXAFS) analysis. Fits were made in the R-space with the k^2-weighted Fourier-transformed EXAFS data. Scanning electron microscopy (SEM) was used to visualize the zeolite crystals using a JEOL JSM-6010LV microscope. The SEM samples were coated with a conductive Au or Pd coating via sputtering before the measurement was executed.

Catalyst loading (CBV-100-Ru(bipy)$_3$) – $Si_{2.55}Al_1O_{7.1}Na_{0.978}Ru_{0.022}$

The catalyst is synthesized within the supercages of the commercially available CBV-100 zeolite via a ship-in-a-bottle method, which is slightly adapted in comparison with literature.[1] First an ion-exchange was performed: 1 g of the zeolite in Na-form was placed into a polypropylene recipient with 0.099 mmol (30.6 mg) $Ru(NH_3)_6Cl_3$ and 50 mL Milli-Q water. The suspension was stirred with a magnetic bar for 24 h and afterwards the crystals were three times washed with Milli-Q water. Next, the crystals were dried overnight under vacuum at room temperature to avoid the formation of the oligomer ruthenium red. In a next step, the zeolite was added into a round bottom flask together with 20 equiv. or 1.98 mmol (309 mg) 2,2'-bipyridine. Subsequently the round bottom flask was immersed in an oil bath at 200 °C for several days, resulting in an orange zeolite powder. The orange zeolite was washed extensively with acetone to remove the excess of 2,2'-bipyridine. Next the material was dried under vacuum overnight and the catalyst was stored in a desiccator.

Arylation reaction

The amination reaction was performed as follows. First, 0.1 mmol (1 equiv; 13 mg) of N-chlorosuccinimide was put into a GC-vial with a magnetic stirring bar and the vial was closed. Via the Schlenk line, the vial was put under inert atmosphere (Ar) and 1 mL of dry 1,1,1,3,3,3-hexafluoro-2-isopropanol (HFIP) or acetonitrile (CH_3CN) was added together with 0.1 mmol (10 µL) of piperidine via a syringe. The vial was placed for 30 min on a magnetic stirrer at room temperature. Subsequently, 2 mol% Ru as CBV-100-Ru(bipy)$_3$ (20 mg CBV-100-Ru(bipy)$_3$) and 18 equiv. or 1.8 mmol (274 µl) t-butylbenzene were added to the vial. Afterwards, 4 equiv. or 0.4 mmol (24 µL) $HClO_4$ was added and the GC-vial was immediately placed for 3 h at room temperature* into the photoreactor (40W blue leds (460-465 nm)). Afterwards 3 mL of ethyl acetate with 0.1 mmol 1,3,5-trimethoxybenzene (external standard) was added to the reaction mixture, centrifuged and analyzed via a GC-FID.

*Not all reactions were executed at room temperature and in some scenarios, the samples were put into a cooling bath to suppress electrophilic aromatic chlorination:

- 0°C: ice in water
- -20°C: dry ice in o-xylene
- -40°C: dry ice in acetonitrile

Reactor

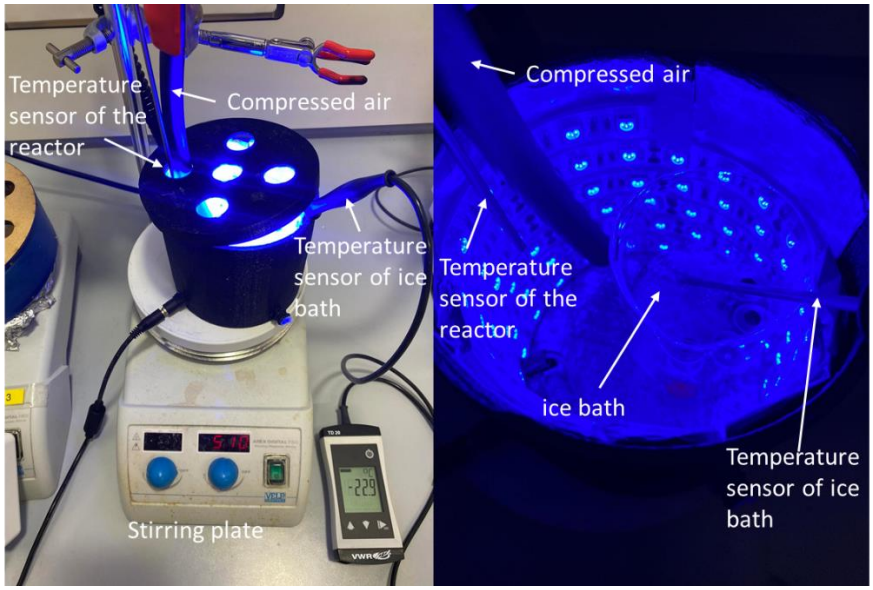

Figure S1: A picture of the reactor. The reactor itself is 3D printed and equipped with a 40 W blue led strip (460-465 nm) inside. The reactor is put on a stirring plate and is provided with a temperature sensor and compressed air to cool the reactor. If necessary, an ice bath equipped with a temperature sensor was placed in the reactor.

2. Catalyst characterization

ICP

Table S1: The Ru-content in the zeolite framework of CBV-100-Ru(bipy)$_3$ determined by ICP-OES analysis. The theoretical Ru-content was also determined knowing that the zeolite was loaded with 1 wt% of ruthenium.

	Ru-content (ppm)	Experimental Ru-content (mg Ru/mg zeolite)	Theoretical Ru content (mg Ru/mg zeolite)	Built-in efficiency
CBV-100-Ru(bipy)$_3$	2.311	0.00911	0.01	**91%**

NMR

From Figure S2, a clear distinction between coordinated and uncoordinated 2,2'-bipyridine is observed, since the peaks are clearly shifted if the ligand is attached to the Ru-atom.

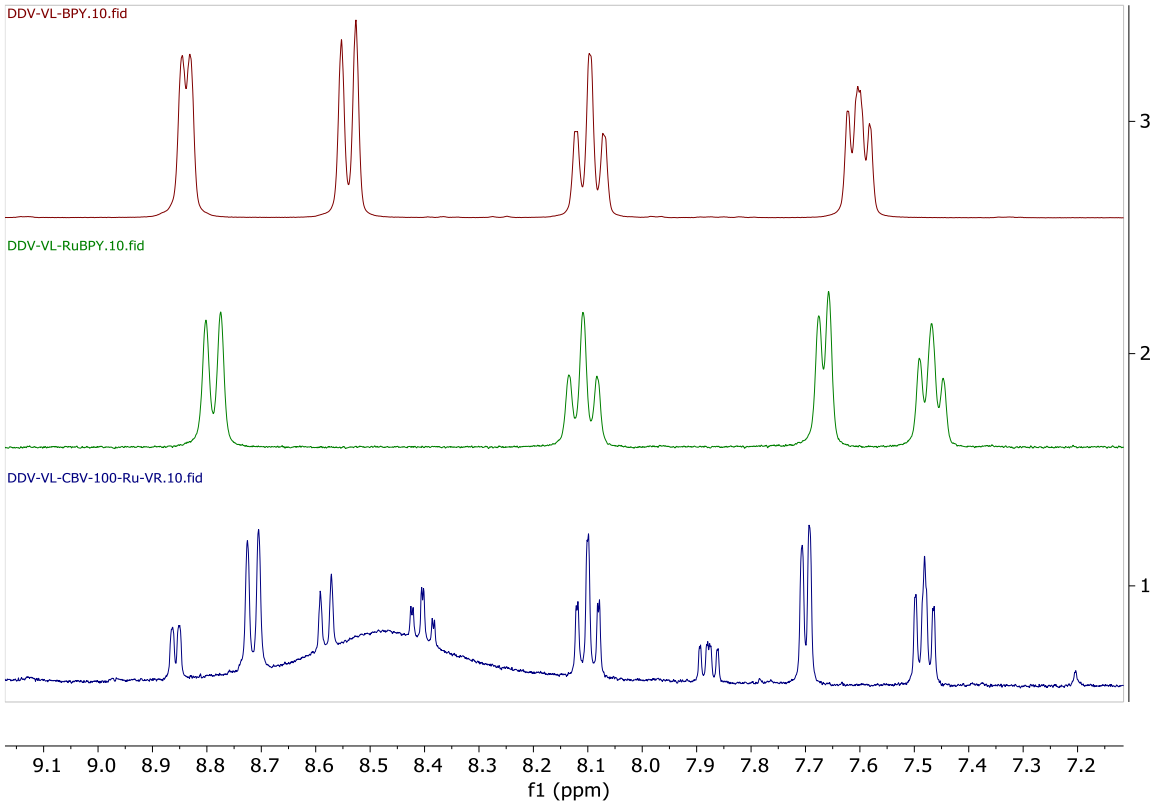

Figure S2: ^{1}H-NMR spectrum of the digested zeolite CBV-100-Ru(bipy)$_3$ (1), Ru(bipy)$_3$Cl$_2$ (2) and 2,2'-bipyridine (3) to determine the difference between coordinated and uncoordinated 2,2'-bipyridine.

Since there is a remarkable difference in peak position (Figure S2), an estimation can be made of the number of ligands that surround the Ru-center. We used following procedure:

1. From ICP-OES data, we determined the amount of Ru per mg of zeolite, which is 0.00911 mg Ru/mg zeolite (Table S1). According to this value, we are able to calculate the amount of 2,2'-bipyridine that surrounds the Ru-ion if it is fully coordinated (i.e. three 2,2'-bipyridine ligands). Consequently, if 3.9 mg of zeolite was digested, the expected amount of coordinated 2,2'-bipyridine is **0.00106 mmol**.
2. To verify if this Ru-ion is indeed coordinated by three ligands, ^{1}H-NMR was performed on 3.9 mg zeolite after digestion and the content of ligand was determined by the addition of an external standard (i.e. 1,3,5-trimethoxybenzene). This is possible, since in Figure S2, a clear distinction can be made between uncoordinated and coordinated bipyridine. By following this method, the amount of coordinated 2,2'-bipyridine from ^{1}H-NMR was estimated at **0.00105 mmol**.

The latter number is remarkably similar to the number expected for a full coordination of the metal. The red-labeled peaks in Figure S3 belong to uncoordinated bipyridine, which originates from leftovers from the ship-in-a-bottle method where an excess of 2,2'-bipyridine is used.

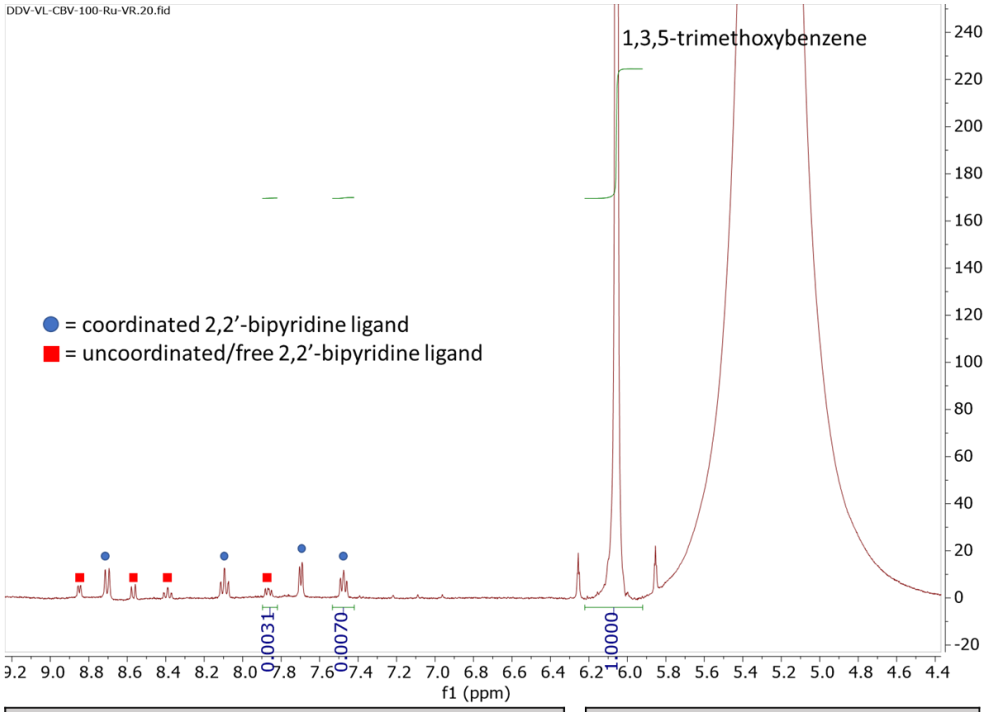

NMR				ICP	
	surface	Surface/H-atoms	mmol	Zeolite	3,9 mg
TMB	1	0.33	0.1	Ru-content	0,035 mg
Free bipy	0.0031	0.0015	0.00046	Ru-content	0.00035 mmol
Coor. bipy	0.0070	0.0035	**0.00105**	bipy-content	**0,00106 mmol**

Figure S3: ^{1}H-NMR spectrum of the digested zeolite CBV-100-Ru(bipy)$_3$ to determine the amount of coordinated and uncoordinated 2,2'-bipyridine. A calculation of the experimental amount of coordinated 2,2'-bipyridine from ^{1}H-NMR and from ICP-OES is determined to check the agreement. TMB = 1,3,5-trimethoxybenzene.

N_2 physisorption

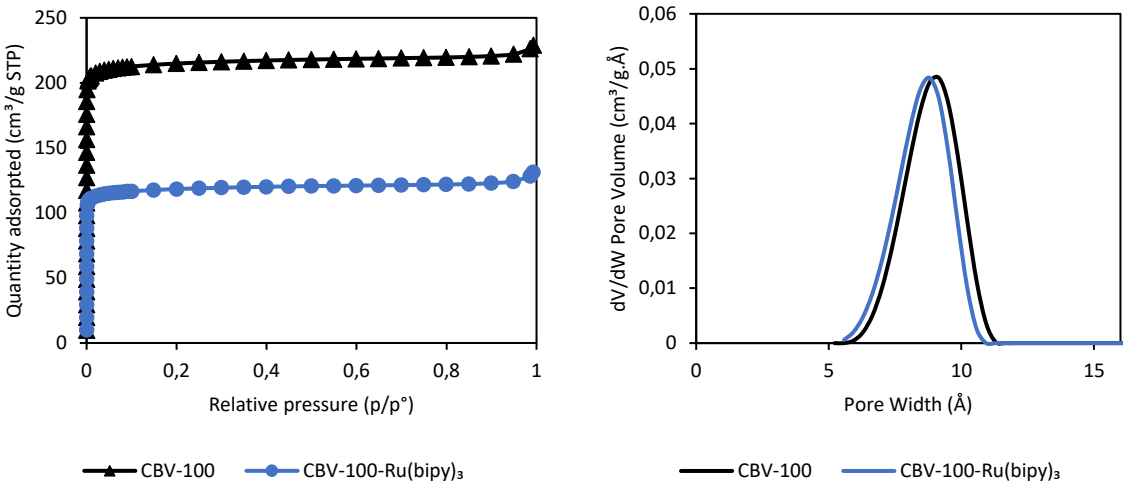

Figure S4: Isotherms and pores size distribution of pristine CBV-100 (black) and $Ru(bipy)_3^{2+}$ containing CBV-100 (blue).

Table S2: The BET and micropore volume of pristine and $Ru(bipy)_3^{2+}$ containing CBV-100.

	BET (m^2/g)	Micropore volume (cm^3/g)
CBV-100	884.9	0.31
CBV-100-Ru(bipy)$_3$	479.2	0.17

SEM

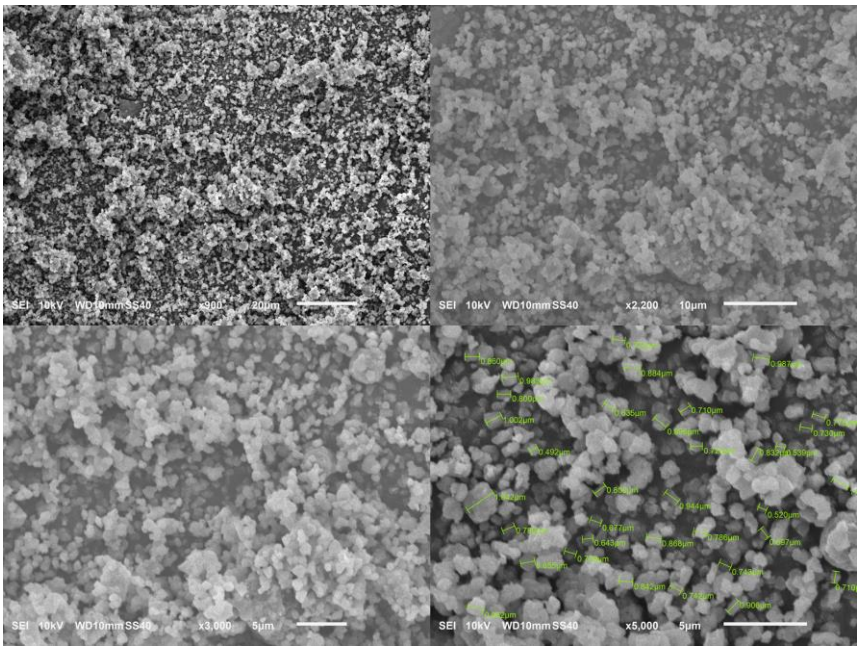

Figure S5: SEM images of CBV-100-$Ru(bipy)_3$ faujasite at different magnifications (x900, x 2200, x3000, x 5000).

FTIR

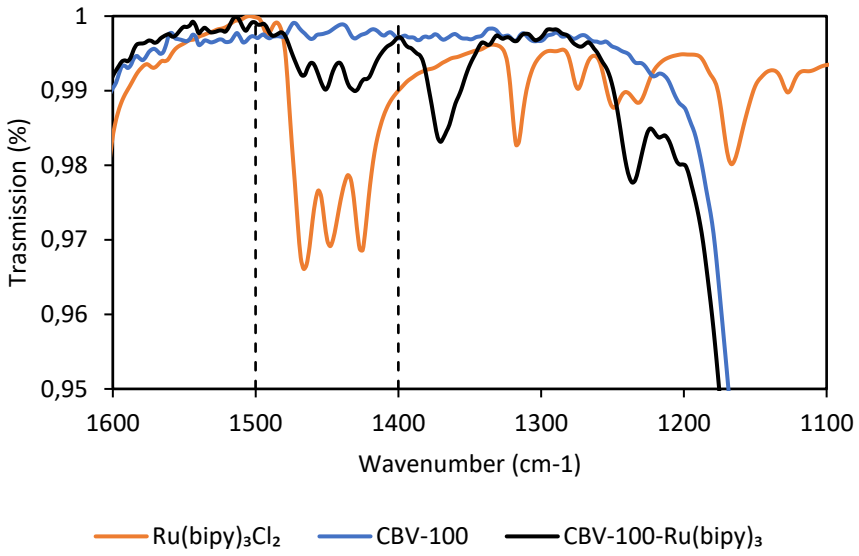

Figure S6: FTIR data for the homogeneous complex ($Ru(bipy)_3Cl_2$, orange), the pristine zeolite (blue) and the $Ru(bipy)_3^{2+}$ impregnated CBV-100-$Ru(bipy)_3$ (black).

XAS

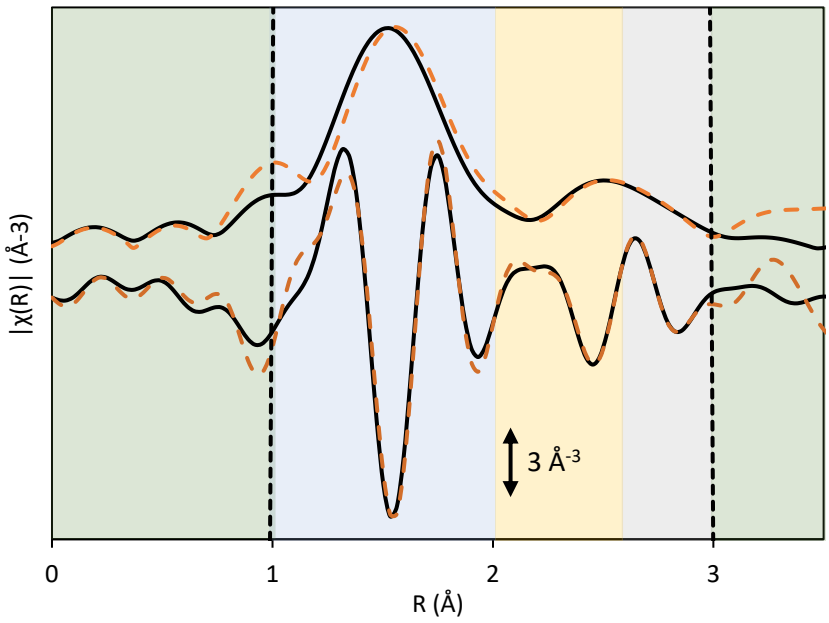

Figure S7: Experimental (solid black) and fitted (dashed red) amplitudes and imaginary parts of the FT-EXAFS data for CBV-100-$Ru(bipy)_3$. Light blue, orange and grey backgrounds highlight the contributions of Ru-N, Ru-C and multiple scattering RU-N-C-Ru paths, respectively. The vertical dashed lines indicate the fitting range.

3. Optimization of the reaction parameters

NMR

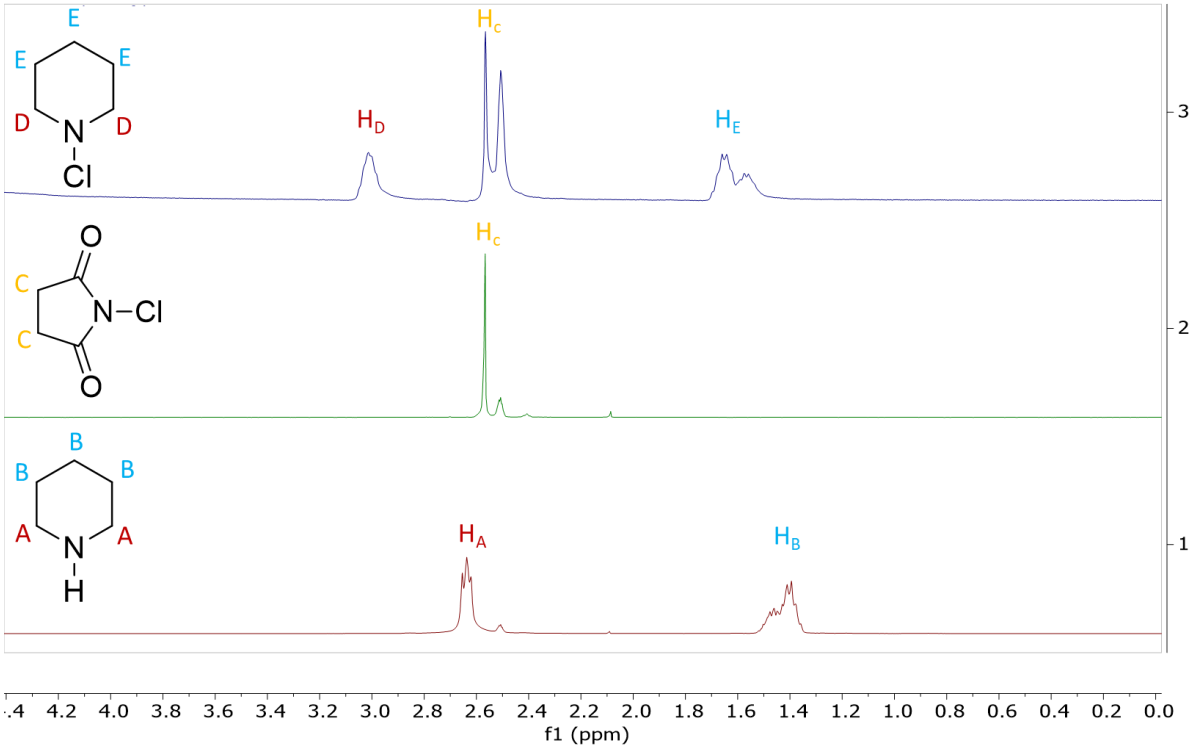

Figure S8: ^{1}H-NMR spectra of piperidine in HFIP (1), N-chlorosuccinimide (NCS) in HFIP (2) and a mixture of N-chlorosuccinimide/piperidine in HFIP (3) to validate the chlorine transfer from NCS to piperidine.

Mechanism

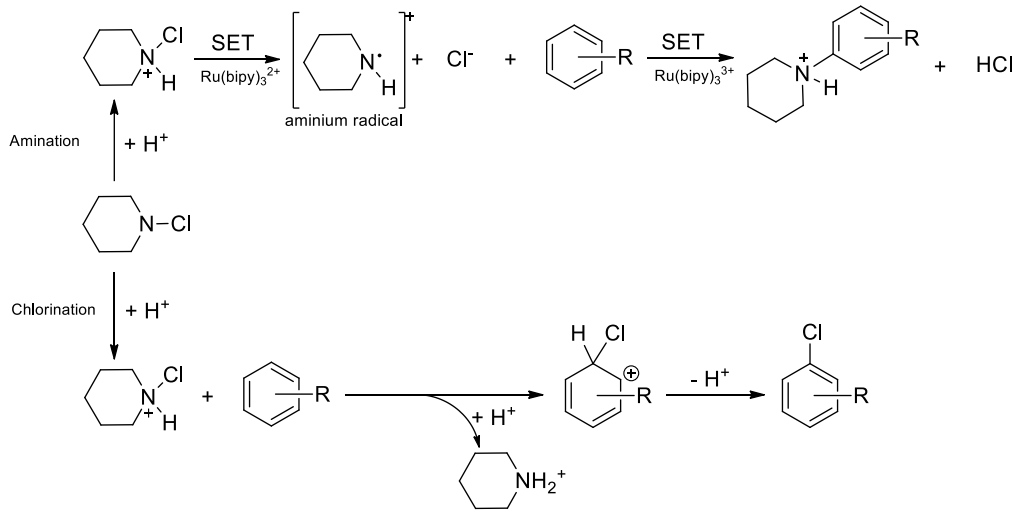

Figure S9: Simplified reaction mechanism of (1) the amination reaction (upper part) and (2) the chlorination reaction (lower part). SET = single electron transfer.

Amount of arene substrate

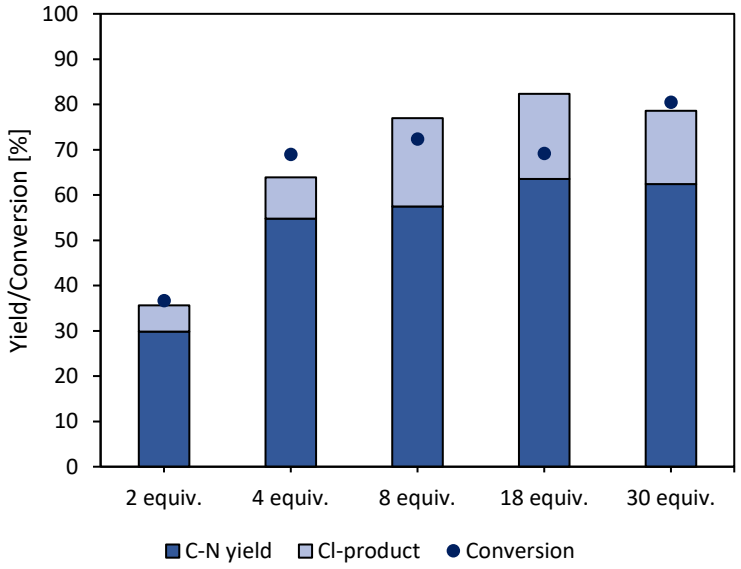

Figure S10: The yield/conversion of reactions with a varying amount of t-butylbenzene (2 equiv., 4 equiv., 8 equiv., 18 equiv. and 30 equiv.). Reaction conditions: 0.1 mmol piperidine, 1 equiv. NCS, ***x equiv. t-butylbenzene****, 4 equiv. $HClO_4$, 1 mL HFIP, 2 mol% Ru as CBV-100-Ru(bipy)$_3$, blue leds, 3h, R.T.*

Acid screening

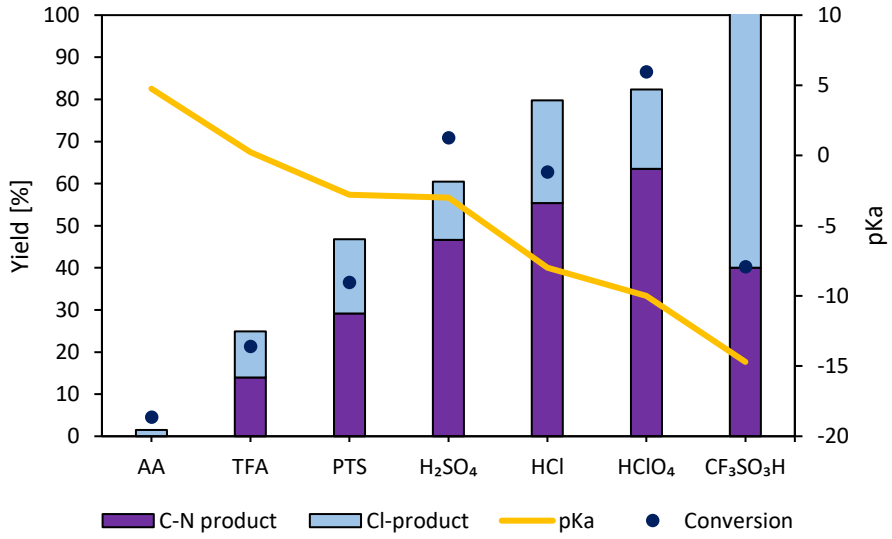

Figure S11: The yield/conversion of reactions with a varying type of (in)organic Bronsted acid (AA = acetic acid, TFA = trifluoroacetic acid and PTS = paratoluene sulfonic acid). Reaction conditions: 0.1 mmol piperidine, 1 equiv. NCS, 18 equiv. t-butylbenzene, ***4 equiv. acid****, 1 mL HFIP, 2 mol% Ru as CBV-100-Ru(bipy)$_3$, blue leds, 3h, R.T.*

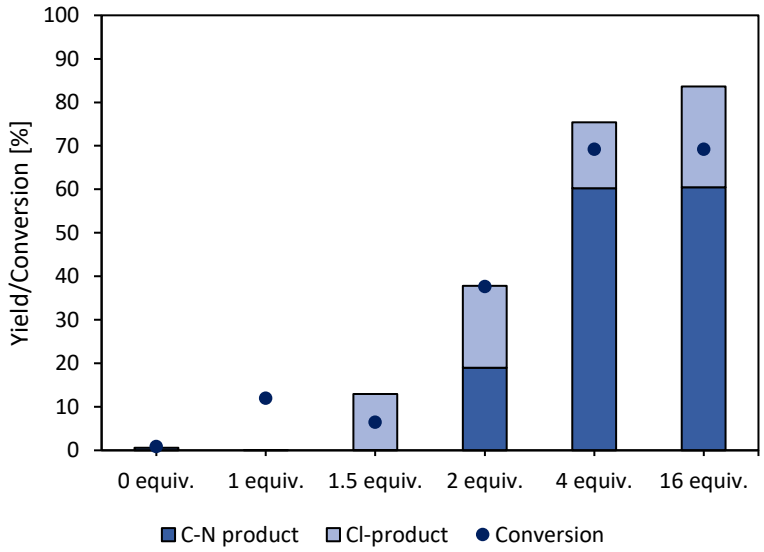

Figure S12: The yield/conversion of reactions with a varying amount of Bronsted acid (0 equiv., 1 equiv., 1.5 equiv., 2 equiv., 4 equiv. and 16 equiv.). Reaction conditions: 0.1 mmol piperidine, 1 equiv. NCS, 18 equiv. t-butylbenzene, ***x equiv. $HClO_4$****, 1 mL HFIP, 2 mol% Ru as CBV-100-Ru(bipy)$_3$, blue leds, 3h, R.T.*

Amount of catalyst

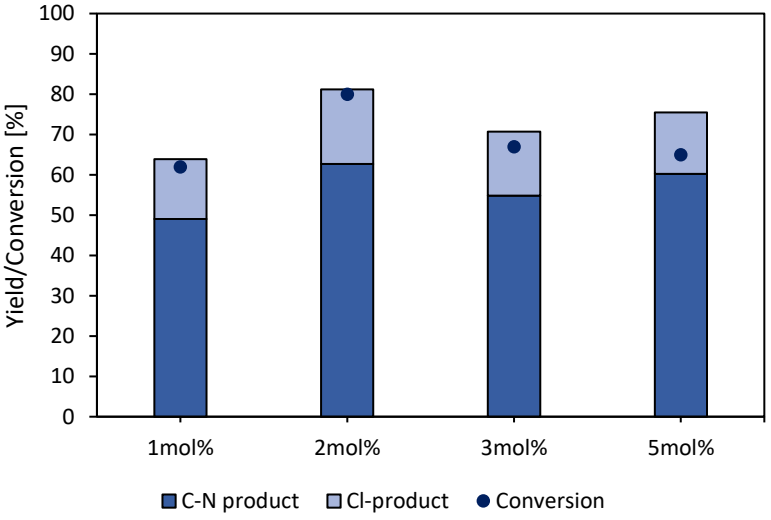

Figure S13: The yield/conversion of reactions with a varying amount of catalyst (1 mol%, 2 mol%, 3 mol% and 5 mol%). Reaction conditions: 0.1 mmol piperidine, 1 equiv. NCS, 18 equiv. t-butylbenzene, 4 equiv. $HClO_4$, 1 mL HFIP, ***x mol% Ru as CBV-100-Ru(bipy)$_3$****, blue leds, 3h, R.T.*

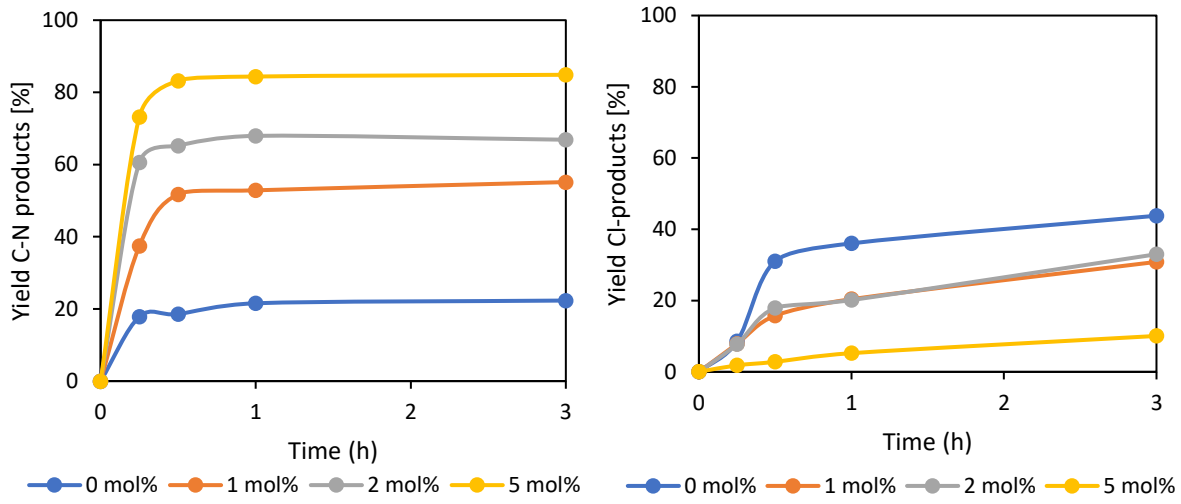

*Figure S14: The yield of C-N product in homogeneous reaction reactions with a varying amount of catalyst (1 mol%, 2 mol%, 3 mol% and 5 mol%) (left). The yield of Cl product in homogeneous reactions with a varying amount of catalyst (1 mol%, 2 mol%, 3 mol% and 5 mol%) (right). Reaction conditions: 0.1 mmol piperidine, 1 equiv. NCS, 18 equiv. t-butylbenzene, 4 equiv. $HClO_4$, 1 mL HFIP, **x mol% $Ru(bipy)_3Cl_2$,** blue leds, 3h, R.T.*

Time analysis

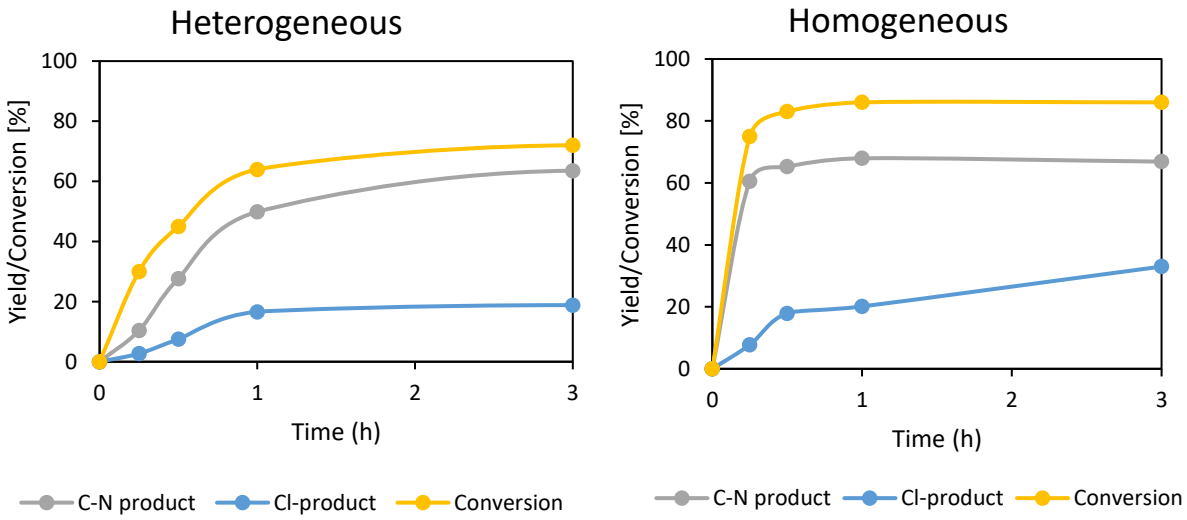

*Figure S15: The yield/conversion of the heterogeneous (left) and homogeneous (right) reaction at multiple time events. Reaction conditions: 0.1 mmol piperidine, 1 equiv. NCS, 18 equiv. t-butylbenzene, 4 equiv. $HClO_4$, 1 mL HFIP, **2 mol% Ru as CBV-100-$Ru(bipy)_3$ (left) or $Ru(bipy)_3Cl_2$ (right)**, blue leds, **x h**, R.T.*

NMR of N-coupling partners

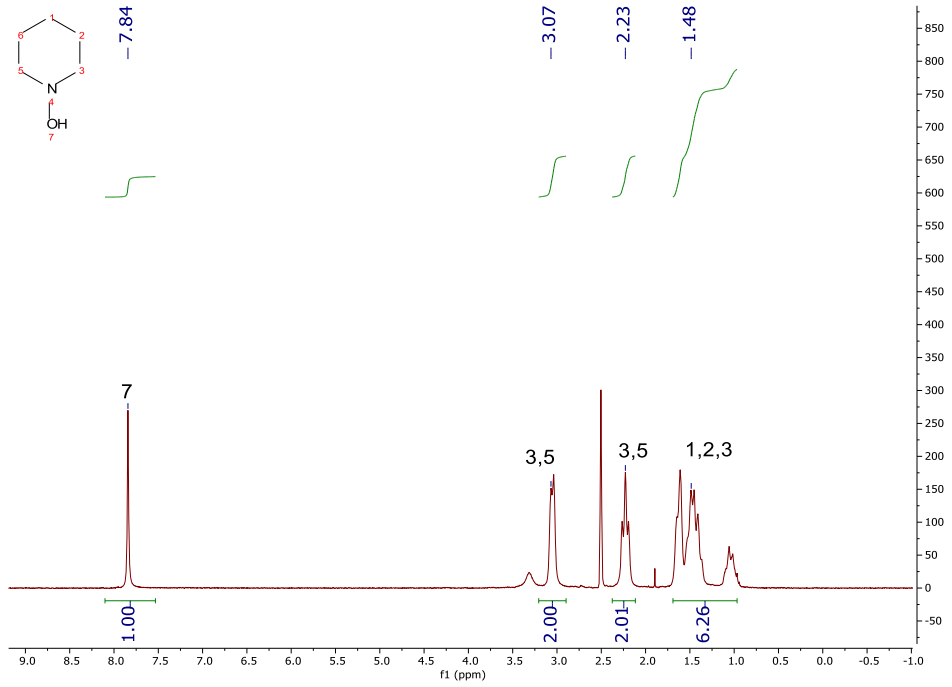

Figure S16: [1]H-NMR spectrum of N-hydroxpiperidine.

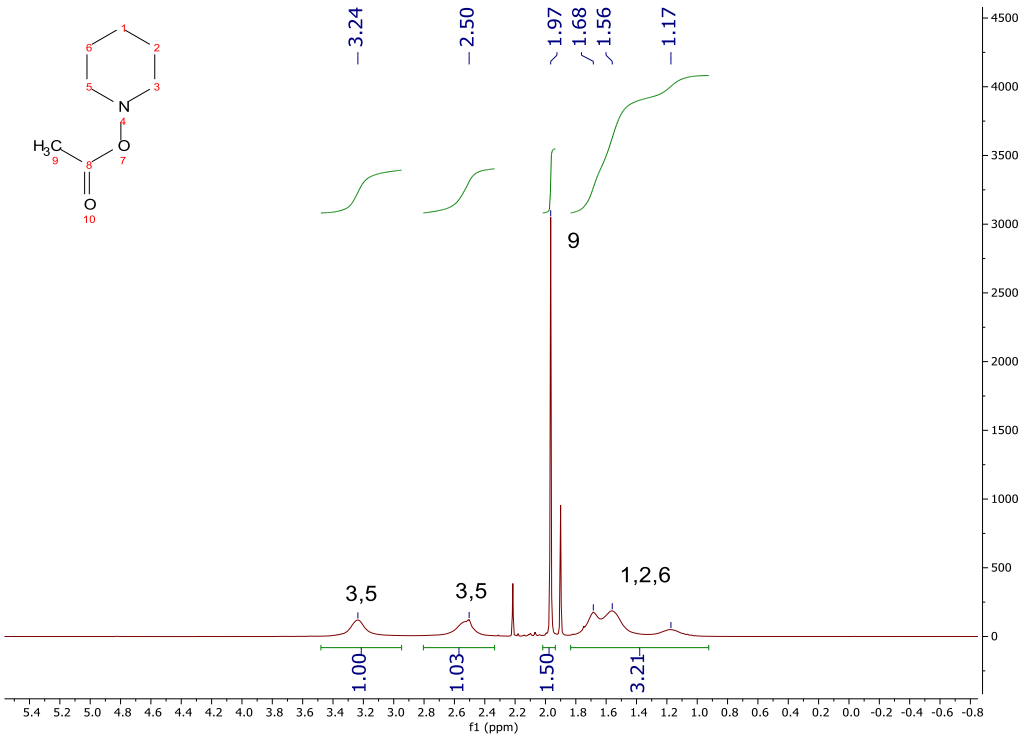

Figure S17: [1]H-NMR spectrum of acetoxy-N-piperidine.[2]

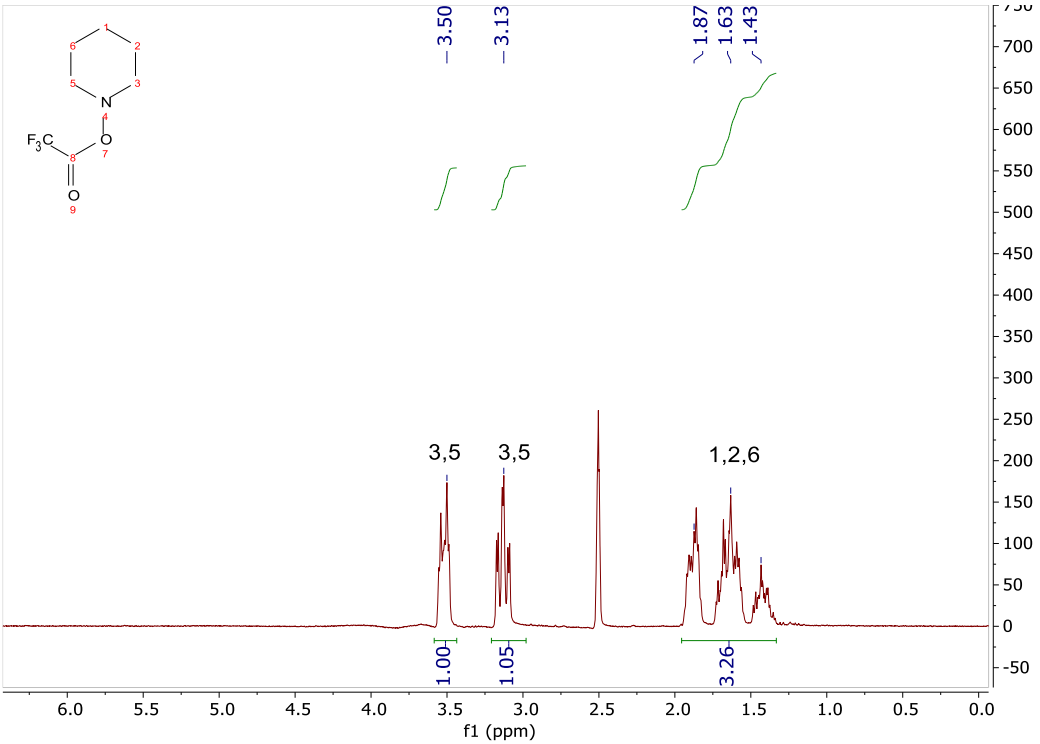

Figure S18: ^{1}H-NMR spectrum of trifluoroacetoxy-N-piperidine.[3]

Support screening

Table S3: The Ru-content in the zeolite framework of different support materials determined by ICP-OES analysis. We expected an amount of 0.01 mg Ru/mg zeolite.

	Ru content (ppm)	Ru content (mg Ru/mg zeolite)
MCM-22-Ru(bipy)$_3$	0.398	0.00156
CBV-100-Ru(bipy)$_3$	**2.311**	**0.00911**
CBV-712-Ru(bipy)$_3$	1.672	0.00666
CBV-720-Ru(bipy)$_3$	2.376	0.00679
CBV-760-Ru(bipy)$_3$	0.834	0.00321
CBV-780-Ru(bipy)$_3$	0.973	0.00354
CBV-901-Ru(bipy)$_3$	0.596	0.00173

Table S4: The amount of leaching of the different catalysts determined by ICP-OES analysis.

	Leaching (ppm)	Leaching (mg Ru/ mg zeolite)	Leaching (%)
Solvent MCM-22	0.85	0.00141	90%
Solvent CBV-100	**0.03**	**0.00004**	**<1%**
Solvent CBV-712	Below detection limit	/	/
Solvent CBV-720	0.013	0.00003	<1%
Solvent CBV-760	Below detection limit	/	/
Solvent CBV-780	Below detection limit	/	/
Solvent CBV-901	0.014	0.00002	<1%

Hammett plot

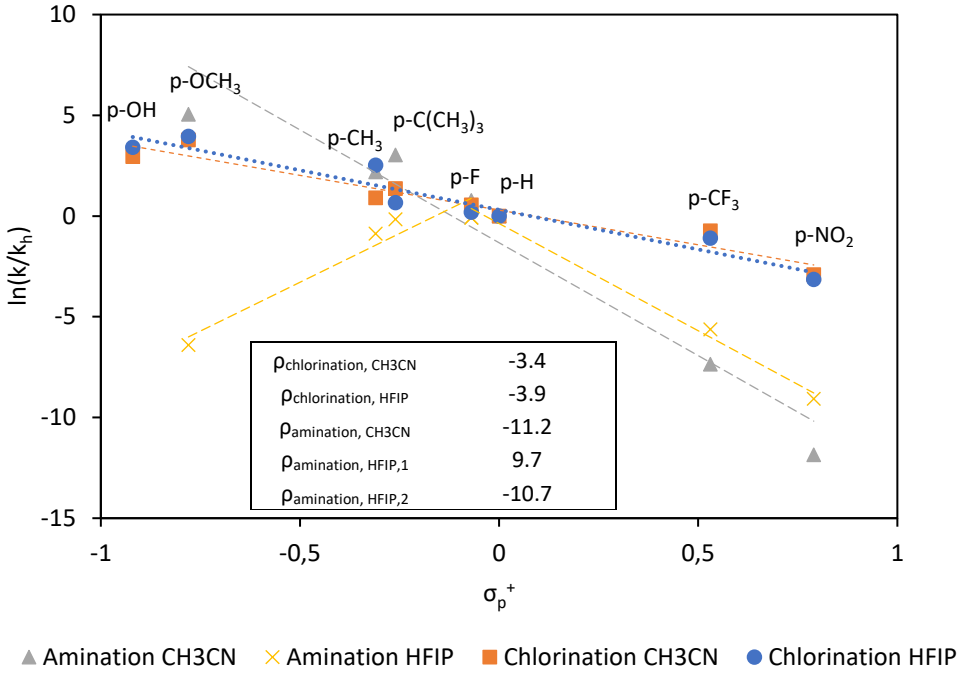

Figure S19: Hammett plots combined in one graph of the homogeneous chlorination and amination reaction in HFIP and CH_3CN. Only the product with the chlorine/amine on the para position are considered in these plots. Reaction conditions: 0.1 mmol piperidine, 1 equiv. NCS, ***18 equiv. arene****, 4 equiv. $HClO_4$, 1 mL HFIP, 2 mol% $Ru(bipy)_3Cl_2$, blue leds, 15 min, R.T.*

Temperature plot

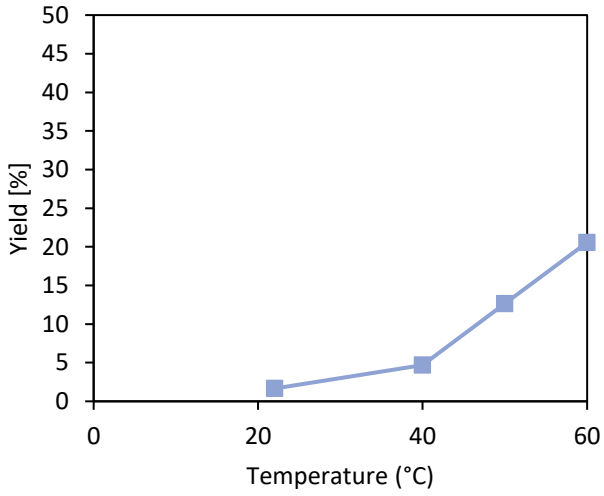

Figure S20: Yield of chlorinated products in the dark reaction at different temperatures (20°C, 40°C, 50°C and 60°C). Reaction conditions: 0.1 mmol piperidine, 1 equiv. NCS, 18 equiv. t-butylbenzene, 4 equiv. $HClO_4$, 1 mL HFIP, 2 mol% Ru as CBV-100-$Ru(bipy)_3$, blue leds, 1h, ***T****.*

4. Heterogeneity tests

XRD

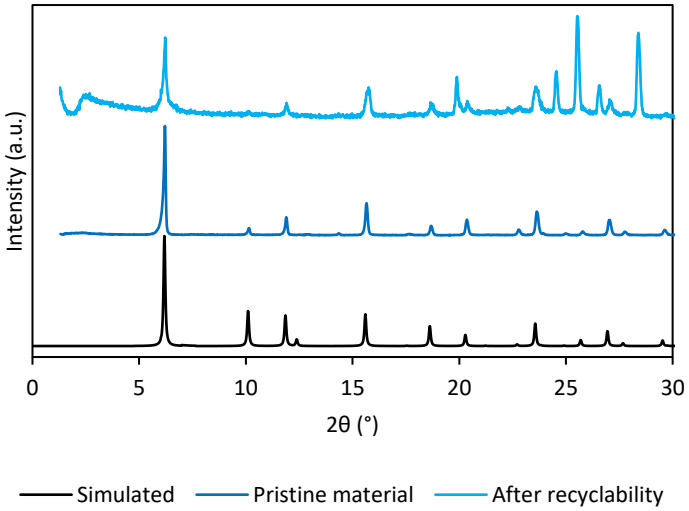

Figure S21: PXRD diffractogram of the simulated CBV-100 (black line), of the pristine CBV-100 (dark blue) and of the loaded CBV-100-Ru(bipy)$_3$ material after four consecutive runs (light blue).

ICP-OES

Table S5: The amount of Ru leaching in the reaction solution after the reaction was performed under the optimized conditions. The values ware determined by ICP-OES and the total amount of leaching after four consecutive runs is measured.

	Leaching (ppm)	Leaching (mg Ru/ mg zeolite)	Leaching (%)
Run 1	0.0825	0.000091	0.99 %
Run 2	Below detection limit	/	/
Run 3	Below detection limit	/	/
Run 4	Below detection limit	/	/
			0.99 %

5. Discussion on sustainability and economy

To gain deeper insight into the sustainability and the economics of our approach, a comparison study is made between our work and other relevant alternatives in the current literature (Table S6) .[4,5,6,7,8,9] In this way, the reactions are easily compared with each other and the negative effects exposed (Table S7).

Table S6: Different relevant strategies for the generation of alkylaminium radical cations for C-H amination.

Nicewicz *et al*.[4]	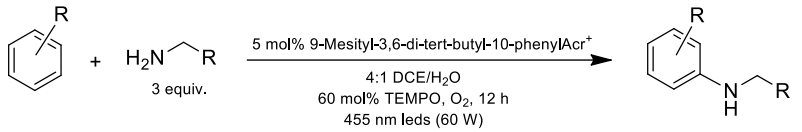
Itoh *et al*.[5]	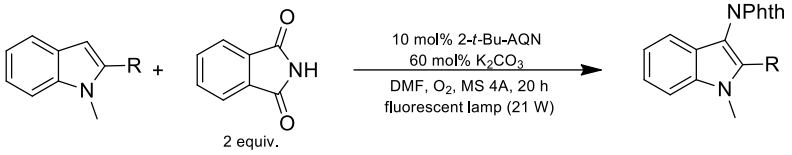
Ooi *et al*.[6]	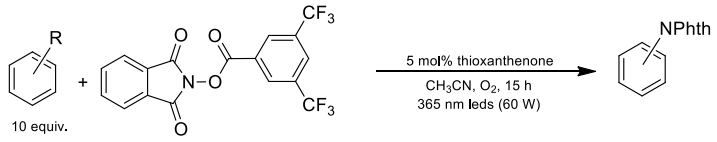
Sanford *et al*.[7]	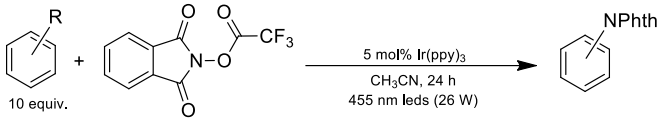
Svejstrup *et al*.[8]	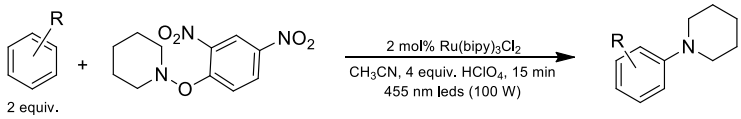
Leonori *et al*.[9]	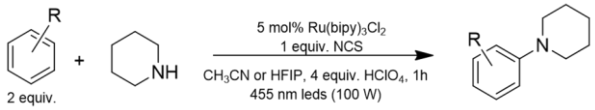
Our work	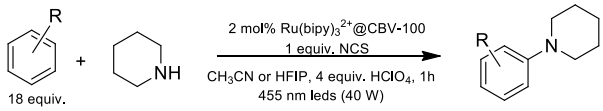

The **reaction yield** is a first indicator, quantifying the amount of product that is formed during the reaction. However, it does not take into account the efficiency of the reaction and is therefore not considered as a real tool to measure the sustainability (Table S7).

The ***E*-factor** on the other hand, as introduced in the early eighties by Roger Sheldon,[10] is a more powerful indicator, since it can easily estimate the impact on the environment. It simply measures the relative amount of waste that is generated during the formation of the product:

$$E - factor = \frac{mass\ of\ the\ waste\ (kg)}{mass\ of\ the\ product\ (kg)}$$

In general, the *E*-factor for all these reaction types (Table S7) is relatively high, since they are performed in very diluted systems using a lot of solvent (as is typical in the pharmaceutical industry). Furthermore, the pre-functionalization steps (e.g. Ooi, Sanford, Svejstrup) have an extremely adverse effect on this *E*-factor. Our approach has a much lower *E*-factor than those reactions requiring pre-functionalization, especially when CH_3CN can be used as solvent (*E*-factor = 65). The **mass intensity** is introduced as a parameter that describes the amount of reagents, solvents, catalysts, addivites,… that are needed to obtain the product and is strongly related to the *E*-factor. This number could also be expressed as the **mass productivity (MP)**, which displays to what extent the raw materials are used.

$$Mass\ intensity\ (MI) = E - factor + 1$$

$$Mass\ productivity\ (MP) = \frac{1}{MI} \times 100$$

In addition, the **atom economy** is defined as the mass of atoms in the desired product divided by the mass of atoms in all reagents. In other words, this number reflects how many atoms of the reagents are used to form the desired product according to the reaction equation. The **carbon efficiency** is more or less similar than the atom economy, but it takes into account the number of carbons that are built in the product . Both parameters are also strongly affected by pre-functionalization steps and therefore our approach, even if NCS is used, is considered as a good alternative regarding the sustainability.

$$Atom\ economy = \frac{MM\ product}{MM\ substrates} \times 100$$

$$Carbon\ efficiency = \frac{carbon\ atoms\ in\ product}{carbon\ atoms\ in\ substrate} \times 100$$

Beside these sustainability parameters, all reactions are also compared on **an economical point of view**. To obtain the electricity cost of these reactions, only the power of the lamps, the duration of the reaction and the estimated electricity price (i.e. €0.74/kWh) need to be taken into account. Since the reports from Svejstrup, Leonori and our work do not require long reaction times, a strong decrease in electricity cost could be observed.

The previous reports are also compared in terms of the cost of the substrates, reagents, catalysts, solvents,… Here, we assume that:

- All reactions are started with 0.1 mol of substrate
- The price for substrate/purification is not considered
- The price of all chemicals were obtained from Sigma Aldrich

A clear distinction between organic and transition metal-based photocatalysts can be made, since the transition-metals are more expensive, which therefore results in slightly higher reaction costs. Furthermore, a comparison between these metals revealed that iridium is by far the most expensive one (Ir = 154 200 €/kg vs Ru = 15 850 €/kg) and this also results in a high price. Although no pre-functionalization step is required in the Leonori approach, the reaction cost compared to Svejstrup is relatively high due to (1) a higher catalyst loading (5 mol% instead of 2 mol%) and (2) the use of HFIP as solvent for some substrates. In our approach, also the main reaction cost is coming from the HFIP solvent, while the catalyst cost could be neglected, since it can be reused for multiple times without significantly

losing its activity. Additionally, for some of our substrates CH_3CN can be used as solvent instead of HFIP and this could result in an enormous economic benefit.

Table S7: Sustainability parameters for the different reaction types. For the Leonori and our approach two different values are given for the E-factor, mass intensity, mass productivity and reaction cost (for 0.1 mol of product), since the reaction can be performed in either HFIP or CH_3CN for suitable substrates.

	Nicewicz[4]	Itoh[5]	Ooi[6]	Sanford[7]	Svejstrup[8]	Leonori[9]		This work	
						HFIP	CH_3CN	HFIP	CH_3CN
Yield (%)	80	82	98	76	61	98	98	**75**	**75**
E-factor	66	53	140	142	207	85	47	**116**	**65**
Mass intensity	67	54	141	143	208	86	48	**117**	**66**
Mass productivity (%)	1.5	1.8	0.7	0.7	0.5	1.3	2.4	**0.9**	**1.5**
Atom economy (%)	99	99	56	86	54	62	62	**62**	**62**
Carbon efficiency (%)	100	100	62	65	71	78	78	**78**	**78**
Energy cost (€)	5.5	3.1	6.7	4.6	0.2	0.4	0.4	**0.8**	**0.8**
Reaction cost (€)	4.3	10.5	3.8	91.3	6.7	18	7.9	**11**	**0.8**

Summarizing, our protocol (together with that of Leonori) offers clear advantages in comparison to the other protocols discussed before and in Table S6, particularly when the reaction is performed in acetonitrile regarding energy cost, reaction cost, E-factor etc. Because of easy catalyst reuse, our protocol is considerably more economical than Leonori's.

With this in mind, the parameters that have a negative influence on the sustainability of our reaction protocol are now within clear view, and they were carefully adapted to obtain more insight (Table S8). Firstly, the amount of substrate in the reaction mixture was increased from 0.1 mmol to 0.5 mmol. Although a lower yield is observed in this scenario, parameters such as E-factor and mass intensity (MI) are strongly reduced, while parallelly mass productivity (MP) increases. In addition, the excess of *t*-butylbenzene is reduced to 10 equiv., while the amount of amine substrate remains similar. In these conditions, a lower yield of 44% is observed (see also Table 1 of the original manuscript). By applying these conditions, small increases in the *E*-factor and mass intensity (MI) are noted due to the lower yield. Consequently, we can conclude that lowering the amount of *t*-butylbenzene does not have a major effect on the sustainability parameters. We added in the supplementary information of our manuscript a discussion on the sustainability and economics and we indicated the changes in yellow in the revised supporting information.

Table S8: Sustainability parameters for our reaction approach using varying conditions. (A) Standard conditions: 0.1 mmol piperidine, 1 equiv. NCS, 18 equiv. t-butylbenzene, 4 equiv. $HClO_4$, 1 mL HFIP, 2 mol% Ru as CBV-100-Ru(bipy)$_3$, blue leds, 3h, R.T. (B) Higher substrate concentration: 0.5 mmol piperidine, 1 equiv. NCS, 18 equiv. t-butylbenzene, 4 equiv. $HClO_4$, 1 mL HFIP, 2 mol% Ru as CBV-100-Ru(bipy)$_3$, blue leds, 3h, R.T. (C) Higher substrate concentration + lower excess of arene: 0.5 mmol piperidine, 1 equiv. NCS, 10 equiv. t-butylbenzene, 4 equiv. $HClO_4$, 1 mL HFIP, 2 mol% Ru as CBV-100-Ru(bipy)$_3$, blue leds, 3h, R.T.

	A: standard conditions	B: Higher substrate concentration	C: Higher substrate concentration +lower excess of arene
Yield (%)	75	60	44
E-factor	116	47	52
Mass intensity	62	62	62
Mass productivity (%)	117	48	53
Atom economy (%)	0.9	2.1	1.9
Carbon efficiency (%)	78	78	78

6. Product identification

Arene substrates

1-(4-(*tert*-butyl)phenyl)piperidine (3a) and 1-(3-(*tert*-butyl)phenyl)piperidine (3a')

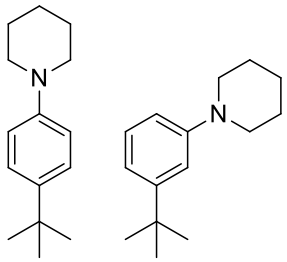

3a **3a'**

Following the general procedure in HFIP at 0°C, **3a** and **3a'** were obtained in 64% and 11%, respectively. Data in accordance with the literature.[8,9]

GC-MS (EI, 70 eV): m/z (rel. int%):
3a: 218 (3), 217 (21), 216 (3), 203 (15), 202 (100), 200 (5), 187 (5), 186 (4), 174 (3), 160 (3), 146 (4), 130 (3), 118 (5), 117 (4), 104 (2), 91 (3), 77 (3), 65 (1), 55 (1), 41 (3)

3a': 218 (16), 217 (100), 216 (14), 203 (2), 202 (11), 200 (6), 186 (2), 176 (9), 160 (7), 146 (17), 130 (4), 118 (7), 117 (7), 104 (4), 91 (7), 77 (5), 65 (2), 57 (3), 41 (6)

^{1}H-NMR (400 MHz, $CDCl_3$), spectra are displayed below and are in accordance with the literature.[8] This data was collected following this procedure; 3 mL EtOAc and 10 mL of 1M KOH was added to the reaction mixture and the layers were separated. The aqueous layer was extracted with EtOAc for two more times and the organic layers were combined, dried with $MgSO_4$, filtered and evaporated. Then column chromatography was performed to obtain the products (eluent = diethyl ether/n-heptaan (1:9)).

3a: δ 7.28 (2H, d), 6.90 (2H, d), 3.15 (4H, t), 1.73 (4H, m), 1.58 (2H, m), 1.31 (9H,s)

3a': δ 7.21 (1H, t), 7.03 (1H, t), 6.90 (1H,d), 6.78 (1H, dd), 3.16 (4H, m), 1.74 (4H, m), 1.59 (2H,m), 1.33 (9H, s)

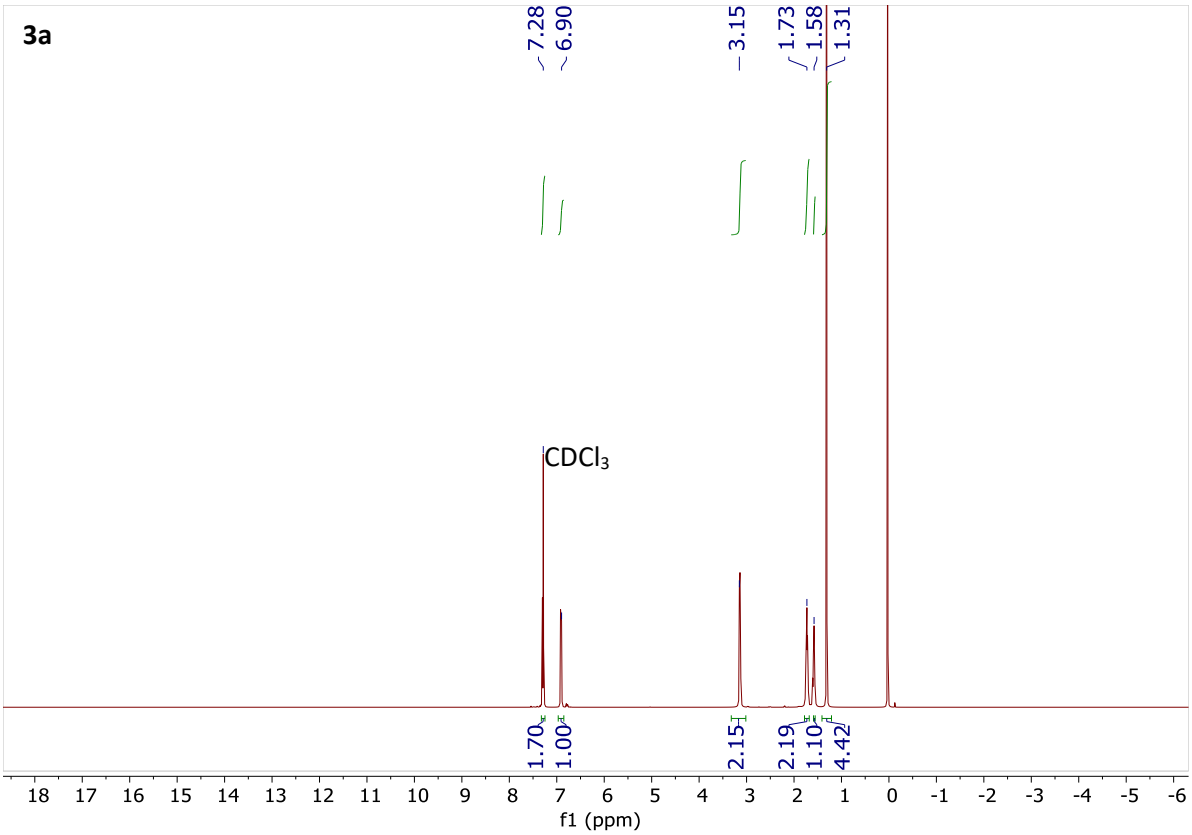
3a
7.28
6.90
3.15
1.73
1.58
1.31
CDCl3
1.70
1.00
2.15
2.19
1.10
4.42
f1 (ppm)

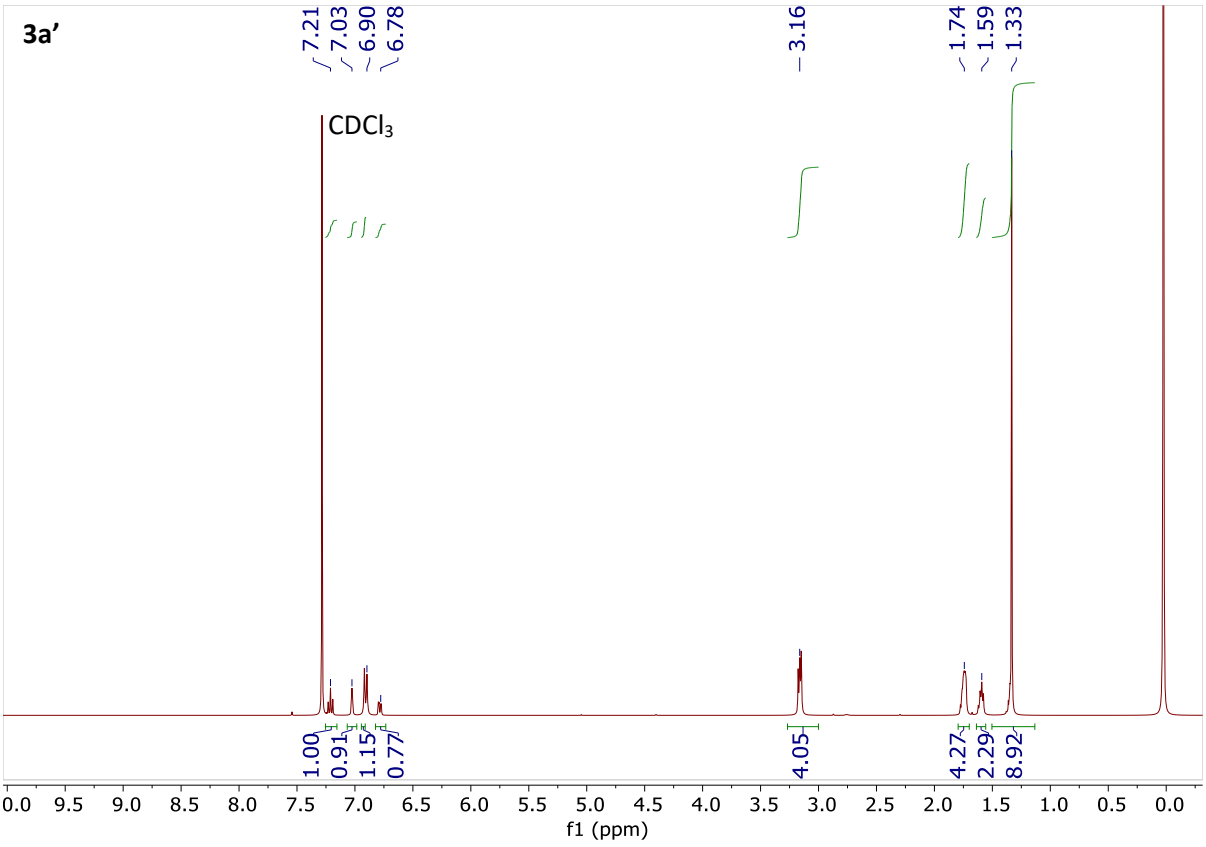
3a'
7.21
7.03
6.90
6.78
3.16
1.74
1.59
1.33
CDCl3
1.00
0.91
1.15
0.77
4.05
4.27
2.29
8.92
f1 (ppm)

1-(4-methoxyphenyl)piperidine (3b) and 1-(2-methoxyphenyl)piperidine (3b')

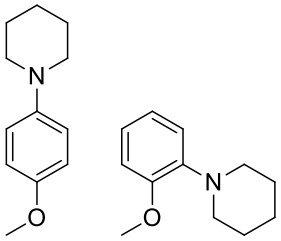

3b **3b'**

Following the general procedure in acetonitrile at -20°C, **3b** and **3b'** were obtained in 47% and 10%, respectively. Data in accordance with the literature.[8,9]

GC-MS (EI, 70 eV): m/z (rel. int%):
3b: 193 (1), 192 (13), 191 (100), 190 (89), 177 (6), 176 (38), 174 (7), 162 (14), 160 (4), 150 (6), 148 (13), 136 (5), 135 (15), 134 (22), 121 (8), 120 (42), 119 (8), 107 (6), 106 (10), 105 (3), 93 (11), 84 (3), 78 (8), 77 (17), 65 (16), 64 (6), 51 (10), 42 (4), 39 (9), 31 (3)

3b': 193 (1),192 (14), 191 (90), 190 (52), 177 (13), 176 (100), 162 (4), 160 (4), 150 (7), 148 (4), 136 (9), 135 (21), 134 (12), 132 (5), 121 (8), 119 (35), 117 (4), 108 (9), 104 (4), 93 (4), 92 (14), 91 (8), 84 (2), 77 (8), 65 (12), 64 (7), 51 (6), 41 (10), 39 (6), 31 (14)

1-(p-tolyl)piperidine (3c) and 1-(m-tolyl)piperidine (3c')

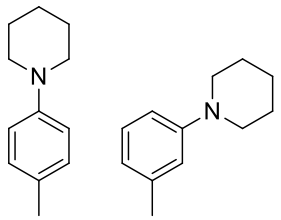

3c **3c'**

Following the general procedure in acetonitrile at -20°C, **3c** and **3c'** were obtained in 47% and 10%, respectively. Data in accordance with the literature.[8,9]

GC-MS (EI, 70 eV): m/z (rel. int%):
3c: 176 (8), 175 (63), 174 (100), 172 (2), 160 (4), 151 (7), 146 (9), 144 (3), 134 (12), 130 (5), 120 (10), 119 (40), 118 (33), 117 (5), 105 (6), 92 (6), 91 (42), 89 (6), 77 (7), 69 (7), 65 (13), 63 (5), 55 (6), 53 (2), 42 (3), 41 (11)

3c': 176 (8), 175 (71), 174 (100), 172 (3), 160 (5), 146 (11), 144 (4), 134 (15), 133 (2), 130 (4), 120 (15), 119 (41), 118 (37), 117 (6), 105 (7), 92 (6), 91 (48), 89 (10), 79 (4), 77 (9), 69 (7), 65 (16), 63 (6), 56 (2) 55 (8), 51 (5), 41 (12)

1-phenylpiperidine (3d)

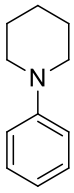

3d

Following the general procedure in HFIP at 0°C, **3d** was obtained in 55%. Data in accordance with the literature.[9]

GC-MS (EI, 70 eV): m/z (rel. int%):
3d: 162 (7), 161 (65), 160 (100), 158 (2), 146 (4), 133 (2), 132 (12), 131 (2), 120 (13), 106 (12), 105 (41), 104 (42), 103 (2), 91 (10), 78 (7), 77 (43), 76 (3), 65 (4), 51 (13), 39 (8)

1-(4-iodophenyl)piperidine (3e)

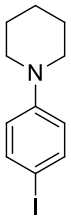

3e

Following the general procedure in HFIP at 0°C, **3e** was obtained in 13%. Data in accordance with the literature.[9]

GC-MS (EI, 70 eV): m/z (rel. int%):
3e: 288 (10), 287 (100), 286 (75), 272 (2), 258 (3), 246 (8), 232 (6), 231 (19), 230 (12), 204 (4), 203 (9), 202 (4), 165 (2), 160 (8), 144 (2), 130 (6), 127 (4), 115 (5), 105 (6), 103 (4), 91 (6), 90 (3), 77 (12), 76 (10), 74 (3), 63 (4), 51 (7), 42 (2), 39 (6)

1-(4-chlorophenyl)piperidine (3f)

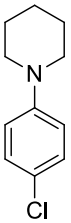

3f

Following the general procedure in HFIP at 0°C, **3f** was obtained in 12%. Data in accordance with the literature.[9]

GC-MS (EI, 70 eV): m/z (rel. int%):
3f: 198 (3), 197 (23), 196 (38), 195 (65), 194 (100), 180 (3), 166 (8), 154 (13), 142 (3), 140 (20), 139 (36),

138 (36), 130 (4), 125 (8), 117 (3), 113 (8), 111 (27), 102 (2), 89 (3), 78 (2), 77 (6), 76 (5), 75 (15), 63 (3), 51 (5), 42 (3), 41 (9)

1-(4-trifluoromethylphenyl)piperidine (3g)

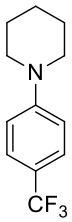

3g

Following the general procedure in HFIP at 0°C, **3g** was obtained in 4%. Data in accordance with the literature.[9]

GC-MS (EI, 70 eV): m/z (rel. int%):
3g: 230 (5), 229 (53), 228 (100), 214 (4), 210 (15), 200 (8), 198 (2), 188 (13), 186 (3), 174 (8), 173 (30), 172 (30), 168 (6), 159 (4), 156 (10), 155 (5), 145 (33), 138 (7), 131 (2), 127 (7), 124 (2), 108 3), 95 (4), 85 (3), 77 (4), 69 (5), 57 (7), 50 (5), 41 (9), 39 (5)

1-(3,4-dimethylphenyl)piperidine (3h)

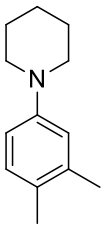

3h

Following the general procedure in acetonitrile at -40°C, **3h** was obtained in 68%. Data in accordance with the literature.[11]

GC-MS (EI, 70 eV): m/z (rel. int%):
3h: 190 (9), 189 (64), 188 (100), 186 (2), 174 (4), 160 (6), 148 (11), 144 (4), 134 (12), 133 (29), 132 (17), 130 (4), 118 (7), 115 (2), 106 (3), 105 (24), 103 (8), 104 (5), 91 (9), 89 (2), 79 (10), 77 (13), 78 (5), 65 (4), 55 (4), 42 (2), 41 (7)

1-(2,4-dimethylphenyl)piperidine (3i)

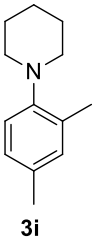

3i

Following the general procedure in acetonitrile at -40°C, **3i** was obtained in 25%. Data in accordance with the literature.[11]

GC-MS (EI, 70 eV): m/z (rel. int%):
3i: 190 (9), 189 (87), 188 (100), 186 (4), 174 (8), 160 (16), 159 (5), 151 (70), 146 (17), 143 (4), 133 (19), 132 (75), 131 (12), 121 (7), 117 (26), 112 (18), 109 (10), 105 (14), 99 (3), 91 (9), 88 (5), 80 (10) 79 (24), 78 (17), 74 (8), 69 (65), 67 (11), 63 (6), 59 (3), 55 (12), 51 (19), 50 (7), 43 (10), 41 (20), 39 (11)

1-(2,5-dimethylphenyl)piperidine (3j)

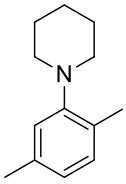

3j

Following the general procedure in acetonitrile at -40°C, **3j** was obtained in 29%. Data in accordance with the literature.[11]

GC-MS (EI, 70 eV): m/z (rel. int%):
3j: 190 (8), 189 (65), 188 (100), 186 (2), 174 (5), 165 (2), 160 (8), 151 (4), 148 (15), 144 (5), 134 (11), 133 (39), 132 (21), 130 (5), 118 (8), 106 (5), 105 (20), 103 (11), 104 (3), 91 (16), 89 (3), 78 (5), 77 (14), 75 (7), 73 (50), 63 (3), 55 (5), 52 (2), 41 (9), 40 (2), 39 (7)

1-(2,4,6-trimethylphenyl)piperidine (3k)

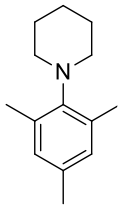

3k

Following the general procedure in acetonitrile at -40°C, **3k** was obtained in 1%. Data in accordance with the literature.[11]

GC-MS (EI, 70 eV): m/z (rel. int%):
3k: 204 (10), 203 (34), 202 (100), 188 (2), 175 (5), 173 (19), 172 (6), 161 (13), 159 (38), 158 (6), 146 (5), 144 (11), 138 (19), 137 (10), 129 (13), 127 (3), 122 (5), 116 (4), 113 (10), 109 (16), 107 (5), 99 (4), 97 (3), 85 (7), 77 (9), 69 (5), 63 (9), 59 (5), 53 (9), 51 (4), 39 (3)

1-(3,4-dimethoxyphenyl)piperidine (3l)

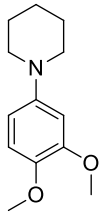

3l

Following the general procedure in acetonitrile at -20°C, **3l** was obtained in 25%. Data in accordance with the literature.[8]

GC-MS (EI, 70 eV): m/z (rel. int%):
3l: 222 (7), 221 (50), 220 (7), 207 (13), 206 (100), 204 (4), 192 (1), 190 (1), 179 (3), 178 (15), 177 (3), 176 (10), 165 (4), 151 (2), 150 (9), 148 (2), 135 (2), 134 (7), 133 (2), 122 (8), 120 (3), 110 (1), 107 (3), 95 (4), 94 (3), 80 (2), 79 (8), 77 (4), 67 (2), 65 (3), 63 (2), 55 (4), 53 (2), 41 (5), 39 (3)

2-(N-methylpyrrole)piperidine (3o) and 3-(N-methylpyrrole)piperidine (3o')

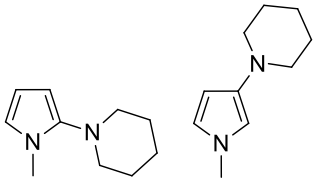

3o **3o'**

Following the general procedure in acetonitrile at -20°C, **3o** and **3o'** were obtained in 19% and 3%, respectively. Data in accordance with the literature.[8,7]

GC-MS (EI, 70 eV): m/z (rel. int%):
3o: 165 (10), 164 (100), 163 (16), 150 (3), 149 (24), 136 (4), 135 (15), 134 (3), 133 (7), 110 (9), 109 (14), 108 (31), 107 (25), 106 (3), 96 (6), 95 (24), 94 (31), 93 (21), 92 (5), 82 (5), 81 (19), 80 (25), 78 (6), 69 (3), 68 (13), 65 (3), 55 (5), 53 (9), 52 (5), 42 (15), 41 (29), 40 (5), 39 (24)

3o': 165 (14), 164 (100), 161 (26), 149 (20), 142 (28), 141 (18), 135 (14), 134 (14), 127 (14), 122 (18), 121 (30), 108 (30), 107 (14), 95 (28), 94 (20), 92 (38), 86 (22), 80 (15), 79 (12), 73 (24), 68 (16), 65 (22), 52 (14), 44 (32), 41 (22), 40 (14), 39 (30)

1-(naphthalen-1-yl)piperidine (3p) and 2-(naphthalen-1-yl)piperidine (3p')

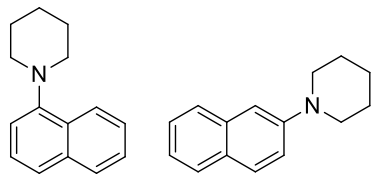

3p **3p'**

Following the general procedure in HFIP at 0°C, **3p** and **3p'** were obtained in 19% and 3%, respectively. Data in accordance with the literature.[8,9]

GC-MS (EI, 70 eV): m/z (rel. int%):
3p: 212 (10), 211 (72), 210 (100), 208 (2), 196 (1), 182 (5), 167 (6), 166 (2), 156 (3), 155 (15), 154 (38), 153 (4), 142 (2), 141 (8), 140 (2), 129 (5), 128 (15), 127 (27), 126 (9), 115 (6), 101 (3), 89 (1), 77 (4), 63 (2), 51 (2), 41 (4)' 39 (4)

3p': 212 (14), 211 (83), 210 (100), 207 (3), 196 (3), 180 (9), 170 (10), 156 (9), 155 (23), 154 (20), 153 (4), 141 (9), 129 (5), 128 (22), 127 (43), 115 (11), 101 (3), 89 (5), 77 (6), 63 (3), 55 (4), 41 (7), 39 (5)

1-(2-methoxy-5-methylphenyl)piperidine (3q) and 1-(3-methoxy-6-methylphenyl)piperidine (3q')

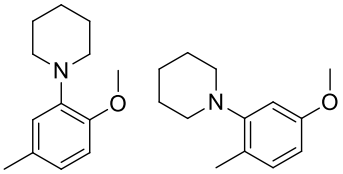

3q **3q'**

Following the general procedure in acetonitrile at -20°C, **3q** and **3q'** were obtained in 20% and 1%, respectively. Data in accordance with the literature.[8,9]

GC-MS (EI, 70 eV): m/z (rel. int%):
3q: 205 (78), 204 (67), 192 (17), 190 (100), 191 (15), 174 (15), 162 (30), 149 (11), 148 (29), 145 (11), 135 (24), 134 (61), 133 (35), 132 (11), 121 (30), 117 (15), 107 (11), 106, (30), 95 (10), 91 (23)), 84 (10), 77 (21), 65 (22), 51 (16), 39 (24)

3q': 205 (100), 204 (65), 190 (50), 174 (16), 164 (40), 148 (75), 133 (40), 128 (82), 121 (35), 117 (10), 107 (12), 104 (50), 94 (50), 92 (13), 44 (25)

1-(3-tert-butyl-tolyl)piperidine (3r)

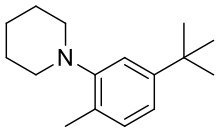

3r

Following the general procedure in HFIP at 0°C, **3r** was obtained in 65%. Data in accordance with the literature.[8,9]

GC-MS (EI, 70 eV): m/z (rel. int%):
3r: 232 (9), 231 (23), 221 (3), 219 (11), 217 (29), 216 (5), 197 (7), 191 (58), 190 (9), 189 (100), 177 (2), 174 (6), 168 (8), 161 (4), 155 (11), 153 (6), 147 (13), 145 (9), 141 (10), 132 (6), 131 (8), 125 (6), 117 (10), 116 (6), 103 (6), 102 (11), 98 (6), 91 (13), 89 (17), 84 (11), 77 (20), 76 (5), 75 (11), 65 (12), 63 (21), 57 (12), 51 (18), 50 (14), 41 (32), 39 (30)

1-(5-iodo-2-methoxyphenyl)piperidine (3s)

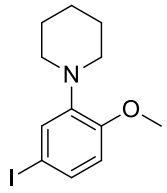

3s

Following the general procedure in HFIP at 0°C, **3s** was obtained in 59%. Data in accordance with the literature.[8,9]

GC-MS (EI, 70 eV): m/z (rel. int%):
3s: 318 (4), 317 (38), 302 (3), 291 (5), 290 (3), 286 (3), 233 (5), 219 (6), 218 (100), 203 (24), 201 (5), 190 (20), 189 (5), 180 (3), 163 (5), 128 (3), 127 (28), 106 (3), 91 (7), 77 (4), 78 (8), 76 (22), 74 (24), 73 (8), 64 (4), 63 (67), 62 (33), 61 (15), 53 (4), 50 (11), 49 (3)

1-(5-bromo-2-methoxyphenyl)piperidine (3t)

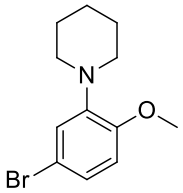

3t

Following the general procedure in HFIP at 0°C, **3t** was obtained in 43%. Data in accordance with the literature.[8,9]

GC-MS (EI, 70 eV): m/z (rel. int%):
3t: 273 (1), 272 (11), 271 (95), 270 (100), 269 (94), 268 (95), 257 (8), 256 (60), (255 (10), 254 (70), 242 (6), 241 (1), 240 (11), 238 (5), 230 (5), 228 (18), 215 (13), 214 (27), 213 (15), 212 (24), 202 (3), 201 (18), 200 (63), 1199 (27), 198 (66), 197 (9), 190 (9), 188 (4), 186 (9), 183 (12), 182 (5), 173 (14), 171 (24), 169 (6), 160 (18), 148 (3), 147 (11), 146 (25), 145 (18), 144 (8), 133 (15), 121 (4), 120 (12), 119 (42), 117 (23), 106 (14), 104 (22), 103 (7), 93 (6), 92 (13), 91 (39), 90 (22), 89 (9), 80 (5), 77 (32), 75 (21), 74 (8), 65 (19), 63 (51), 55 (45), 54 (9), 51 (36), 43 (5), 42 (21), 41 (71), 40 (9), 39 (47)

Nitrogen coupling partners

1-(4-(*tert*-butyl)phenyl)piperidine (4a) and 1-(3-(*tert*-butyl)phenyl)piperidine (4a')

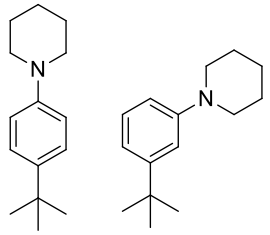

4a **4a'**

Following the general procedure in HFIP at 0°C, **4a** and **4a'** were obtained in 64% and 11%, respectively. Data in accordance with the literature.[9]

GC-MS (EI, 70 eV): m/z (rel. int%):
4a: 218 (3), 217 (21), 216 (3), 203 (15), 202 (100), 200 (5), 187 (5), 186 (4), 174 (3), 160 (3), 146 (4), 130 (3), 118 (5), 117 (4), 104 (2), 91 (3), 77 (3), 65 (1), 55 (1), 41 (3)

4a': 218 (16), 217 (100), 216 (14), 203 (2), 202 (11), 200 (6), 186 (2), 176 (9), 160 (7), 146 (17), 130 (4), 118 (7), 117 (7), 104 (4), 91 (7), 77 (5), 65 (2), 57 (3), 41 (6)

1-(4-(*tert*-butyl)phenyl)pyrrolidine (4b) and 1-(3-(*tert*-butyl)phenyl)pyrrolidine (4b')

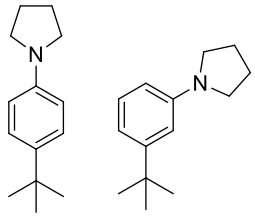

4b **4b'**

Following the general procedure in HFIP at 0°C, **4b** and **4b'** were obtained in 47% and 11%, respectively. Data in accordance with the literature.[9]

GC-MS (EI, 70 eV): m/z (rel. int%):
4b: 204 (4), 203 (22), 202 (3), 189 (16), 188 (100), 186 (8), 174 (1), 173 (8), 172 (5), 160 (4), 147 (2), 146 (4), 131 (3), 117 (5), 116 (2), 103 (2), 94 (1), 91 (5), 77 (3), 65 (1), 51 (1), 41 (3)

4b': 204 (13), 203 (87), 202 (100), 189 (4), 188 (25), 187 (7), 172 (4), 160 (10), 148 (4), 147 (22), 146 (10), 144 (4), 132 (2), 131 (5), 119 (3), 118 (5), 117 (8), 116 (4), 115 (8), 103 (3), 94 (2), 91 (11), 89 (3), 77 (7), 78 (2), 65 (3), 57 (2), 51 (3), 41 (6), 39 (4)

1-(4-(*tert*-butyl)phenyl)morpholine (4c) and 1-(3-(*tert*-butyl)phenyl)morpholine (4c')

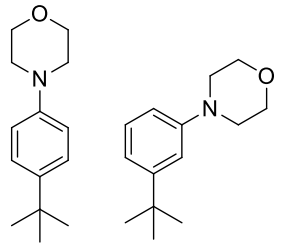

4c **4c'**

Following the general procedure in HFIP at 0°C, **4c** and 4c**'** were obtained in 8% and 1%, respectively. Data in accordance with the literature.[9]

GC-MS (EI, 70 eV): m/z (rel. int%):
4c: 219 (15), 218 (6), 207 (11), 205 (8), 204 (100), 198 (4), 194 (6), 188 (5), 171 (3), 168 (11), 161 (18), 159 (5), 141 (6), 139 (10), 133 (4), 122 (10), 115 (6), 104 (6), 96 (8), 93 (11), 87 (6), 77 (8), 69 (22), 63 (15), 60 (11), 57 (8), 55 (4), 47 (3), 45 (23), 42 (7)

4c': 219 (29), 205 (8), 204 (100), 202 (2), 189 (3), 160 (5), 159 (4), 158 (2), 146 (8), 145 (5), 144 (3), 132 (8), 131 (8), 130 (6), 118 (8), 117 (4), 115 (9), 91 (3), 77 (5)

1-(4-(*tert*-butyl)phenyl)-4-hydroxypiperidine (4d) and 1-(3-(*tert*-butyl)phenyl)-4-hydroxypiperidine (4d')

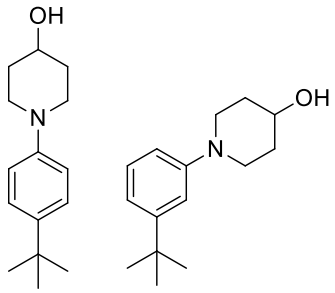

4d **4d'**

Following the general procedure in HFIP at 0°C, **4d** and **4d'** were obtained in 36% and 8%, respectively. Data in accordance with the literature.[9]

GC-MS (EI, 70 eV): m/z (rel. int%):
4d: 234 (9), 233 (25), 231 (4), 219 (13), 218 (100), 213 (4), 203 (3), 193 (2), 190 (5), 182 (2), 172 (3), 161 (2), 160 (7), 158 (3), 148 (3), 146 (14), 144 (9), 140 (1), 132 (3), 131 (4), 128 (7), 118 (11), 117 (7), 113 (1), 105 (4), 103 (8), 104 (4), 91 (11), 89 (7), 79 (3), 78 (7), 77 (10), 75 (4), 65 (4), 57 (7), 51 (8), 44 (17), 41 (10)

4d': 234 (7), 233 (20), 232 (4), 219 (18), 218 (100), 214 (3), 212 (5), 200 (3), 190 (5), 184 (3), 176 (5), 162 (3), 160 (5), 147 (3), 146 (14), 144 (6), 142 (3), 132 (6), 128 (4), 123 (2), 118 (15), 115 (8), 106 (3), 104 (5), 99 (2), 91 (11), 86 (4), 77 (9), 75 (5), 70 (2), 65 (4), 57 (11), 55 (7), 53 (4), 44 (13), 42 (6), 41 (11)

1-(4-(*tert*-butyl)phenyl)-3,5-dimethylpiperidine (4e) and 1-(3-(*tert*-butyl)phenyl)-3,5-dimethylpiperidine (4e')

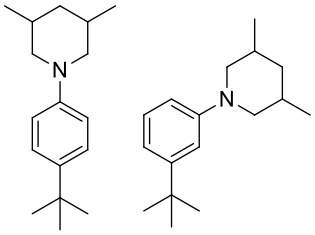

4e **4e'**

Following the general procedure in HFIP at 0°C, **4e** and **4e'** were obtained in 36% and 8%, respectively. Data in accordance with the literature.[9]

GC-MS (EI, 70 eV): m/z (rel. int%):
4e: 246 (4), 245 (21), 244 (3), 231 (18), 230 (100), 228 (2), 214 (3), 202 (2), 188 (2), 176 (2), 170 (1), 161 (2), 147 (3), 146 (15), 145 (3), 143 (1), 130 (5), 119 (2), 118 (9), 117 (7), 106 (3), 102 (2), 91 (6), 77 (4), 69 (3), 56 (2), 55 (5), 41 (8)

4e': 246 (4), 245 (19), 244 (3), 231 (19), 230 (100), 228 (2), 215 (2), 202 (4), 188 (2), 176 (3), 162 (1), 161 (4), 147 (5), 146 (22), 144 (4), 132 (4), 118 (14), 117 (11), 116 (5), 115 (8), 105 (4), 104 (6), 91 (9), 89 (2), 77 (8), 69 (5), 65 (2), 55 (8), 41 (17)

1-(4-(*tert*-butyl)phenyl)-2,6-dimethylpiperidine (4f) and 1-(3-(*tert*-butyl)phenyl)-2,6-dimethylpiperidine (4f')

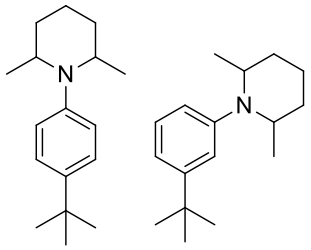

4f **4f'**

Following the general procedure in HFIP at 0°C, **4f** and **4f'** were obtained in 0.1% and 0.1%, respectively. Data in accordance with the literature.[9]

GC-MS (EI, 70 eV): m/z (rel. int%):
4f: 245 (10), 231 (19), 230 (100), 216 (3), 202(1), 188 (2), 179 (2), 175 (5), 167 (2), 161 (4), 160 (21), 158 (4), 150 (1), 144 (6), 134 (3), 131 (3), 130 (5), 118 (6), 117 (15), 115 (8), 111 (1), 106 (5), 98 (3), 91 (16), 90 (3), 79 (4), 77 (7), 72 (2), 65 (4), 57 (6), 55 (17), 52 (2), 44 (4), 43 (7), 42 (10), 41 (14), 39 (8)

4f': 245 (11), 232 (4), 230 (100), 223 (7), 214 (7), 207 (2), 200 (6), 198 (2), 190 (11), 188 (5), 177 (2), 174 (7), 173 (2), 160 (10), 161 (6), 144 (10), 143 (5), 132 (8), 131 (15), 127 (4), 120 (7), 117 (8), 115 (12), 109 (5), 104 (13), 99 (5), 98 (9), 91 (21), 84 (4), 79 (7), 78 (14), 77 (6), 71 (10), 63 (5), 56 (9), 55 (14), 51 (11), 45 (5), 44 (16), 43 (15), 41 (23)

7. References

1. DeWilde W, Peeters G, Lunsford JH. Synthesis and Spectoscopic Properties of Tris(2,2'-bipyridine)ruthenium(II) in Zeolite Y. *J Phys Chem*. Published online 1980:2306-2310.

2. Zhang Z, Yu Y, Liebeskind LS. N-amidation by copper-mediated cross-coupling of organostannanes or boronic acids with O-acetyl hydroxamic acids. *Org Lett*. 2008;10(14):3005-3008. doi:10.1021/ol8009682

3. Kerkovius JK, Menard F. A Practical Synthesis of 6,8-Difluoro-7-hydroxycoumarin Derivatives for Fluorescence Applications. *Synth*. 2016;48(11):1622-1629. doi:10.1055/s-0035-1561603

4. Margrey KA, Levens A, Nicewicz DA. Direct Aryl C À H Amination with Primary Amines Using Organic Photoredox Catalysis Angewandte. Published online 2017:15644-15648. doi:10.1002/anie.201709523

5. Yamaguchi T, Yamaguchi E, Itoh A. Cross-Dehydrogenative C − H Amination of Indoles under Aerobic Photo-oxidative Conditions. Published online 2017:10-13. doi:10.1021/acs.orglett.7b00026

6. Article E, Tripathi CB, Ooi T, Corbett MT. Chemical Science imidation and acyloxylation of arenes †. 2017;(c):5622-5627. doi:10.1039/c7sc01700f

7. Allen LJ, Cabrera PJ, Lee M, Sanford MS. N-acyloxyphthalimides as nitrogen radical precursors in the visible light photocatalyzed room temperature C-H amination of arenes and heteroarenes. *J Am Chem Soc*. 2014;136(15):5607-5610. doi:10.1021/ja501906x

8. Svejstrup TD, Ruffoni A, Juliá F, Aubert VM, Leonori D. Synthesis of Arylamines via Aminium Radicals. *Angew Chemie - Int Ed*. 2017;56(47):14948-14952. doi:10.1002/anie.201708693

9. Ruffoni A, Juliá F, Svejstrup TD, McMillan AJ, Douglas JJ, Leonori D. Practical and regioselective amination of arenes using alkyl amines. *Nat Chem*. 2019;11(5):426-433. doi:10.1038/s41557-019-0254-5

10. Sheldon RA. The: E factor 25 years on: The rise of green chemistry and sustainability. *Green Chem*. 2017;19(1):18-43. doi:10.1039/c6gc02157c

11. Tang RJ, Retailleau P, Milcent T, Crousse B. Direct amination of arenes with azodicarboxylates catalyzed by bisulfate salt/HFIP association. *ACS Omega*. 2019;4(5):8960-8966. doi:10.1021/acsomega.9b00781